Current Biology, Vol. 13, 618–626, April 15, 2003, ©2003 Elsevier Science Ltd. All rights reserved. DOI 10.1016/S0960-9822(03)00207-0

Dendrites of Distinct Classes of *Drosophila* Sensory Neurons Show Different Capacities for Homotypic Repulsion

Wesley B. Grueber,[1] Bing Ye,[1] Adrian W. Moore, Lily Y. Jan, and Yuh Nung Jan*
Howard Hughes Medical Institute
Departments of Physiology and Biochemistry
533 Parnassus Avenue
Room U226
University of California, San Francisco
San Francisco, California 94143

Summary

Backgound: Understanding how dendrites establish their territory is central to elucidating how neuronal circuits are built. Signaling between dendrites is thought to be important for defining their territories; however, the strategies by which different types of dendrites communicate are poorly understood. We have shown previously that two classes of *Drosophila* peripheral da sensory neurons, the class III and class IV neurons, provide complete and independent tiling of the body wall. By contrast, dendrites of class I and class II neurons do not completely tile the body wall, but they nevertheless occupy nonoverlapping territories.
Results: By developing reagents to permit high-resolution studies of dendritic tiling in living animals, we demonstrate that isoneuronal and heteroneuronal class IV dendrites engage in persistent repulsive interactions. In contrast to the extensive dendritic exclusion shown by class IV neurons, duplicated class III neurons showed repulsion only at their dendritic terminals. Supernumerary class I and class II neurons innervated completely overlapping regions of the body wall, and this finding suggests a lack of like-repels-like behavior.
Conclusions: These data suggest that repulsive interactions operate between morphologically alike dendritic arbors in *Drosophila*. Further, *Drosophila* da sensory neurons appear to exhibit at least three different types of class-specific dendrite-dendrite interactions: persistent repulsion by all branches, repulsion only by terminal dendrites, and no repulsion.

Introduction

For a complete and accurate sampling of sensory or presynaptic input, neuronal ensembles can organize as tiled systems, with the dendritic fields of like neurons partitioning a receptive area much like tiles covering a floor. Certain common themes have emerged from studies of very divergent tiled systems. First, neurons of a particular functional or morphological type, such as retinal ganglion cell (RGC) and amacrine cell subtypes [1–6] and insect dendritic arborization (da) neurons [7], are often arranged in an even-spaced mosaic across a receptive territory. Second, dendrites of neighboring neurons fill the area between cell bodies and, in so doing, overlap minimally with each other. These properties together allow for a complete and highly economical coverage of two-dimensional receptive domains and may be applicable to complex systems such as the mammalian cerebral cortex [8].

Studies of the mechanisms of retinal tiling have shown an essential role for interactions between like dendrites. A lesion of a patch of RGCs, for example, leads to dendritic growth of surrounding neurons toward the depleted area [9–12]. However, class-specific differences in the precision of tiling suggest that the nature of dendritic exclusion may vary with cell type. Some ganglion cell subtypes, such as the α cells, consistently show some degree of dendritic overlap [2], while others, such as the direction-selective neurons, show strict dendritic exclusion [4]. Different patterns of tiling might allow a level of anatomical overlap and redundancy that is appropriate or permissible for the physiological function being processed.

Recently, dendritic tiling has been reported in the *Drosophila* peripheral nervous system [7], which provides a potentially useful system for further mechanistic and genetic dissection of this phenomenon. Four morphological classes of dendritic arborization (da) [13] sensory neurons, namely, class I–IV neurons, show different types of dendritic exclusion. The dendrites of class III and IV neurons tile the body wall completely and independently, while classes I and II do not provide complete segmental coverage but nevertheless extend dendrites to innervate nonoverlapping territories. Previous studies indicated that dendritic competition exists between homologous dorsal clusters at the dorsal midline [14] and that dendritic interactions may occur in a class-specific manner between class III neurons and between class IV neurons [7]. Still, it is unknown whether dendrodendritic interactions act generally to shape the territories innervated by various da neurons.

To address the generality of tiling and also its mechanistic basis, we first generated a strain of flies with all class IV neurons marked with Enhanced Green Fluorescent Protein (EGFP) to facilitate live imaging of tiling dendritic arbors. We then combined addition-of-neuron and cell ablation experiments to show that tiling involves repulsive interactions between heteroneuronal dendrites, and also that different classes of neurons differ in their ability to exclude like dendrites. These results reveal an unanticipated diversity in the nature of dendritic interactions between da neurons. Our data suggest a scenario in which a combination of cell intrinsic capacity for growth and growth restriction by inhibitory interplay with like dendrites sculpts the territories of da neurons.

Results

Characterization of Tiling in Living *Drosophila* Larvae by Using an Enhancer-*EGFP* Fusion Construct

Previous studies of tiling in *Drosophila* (Figure 1) [7] relied on the generation of random clones of da neurons

*Correspondence: ynjan@itsa.ucsf.edu
[1]These authors contributed equally to this study.

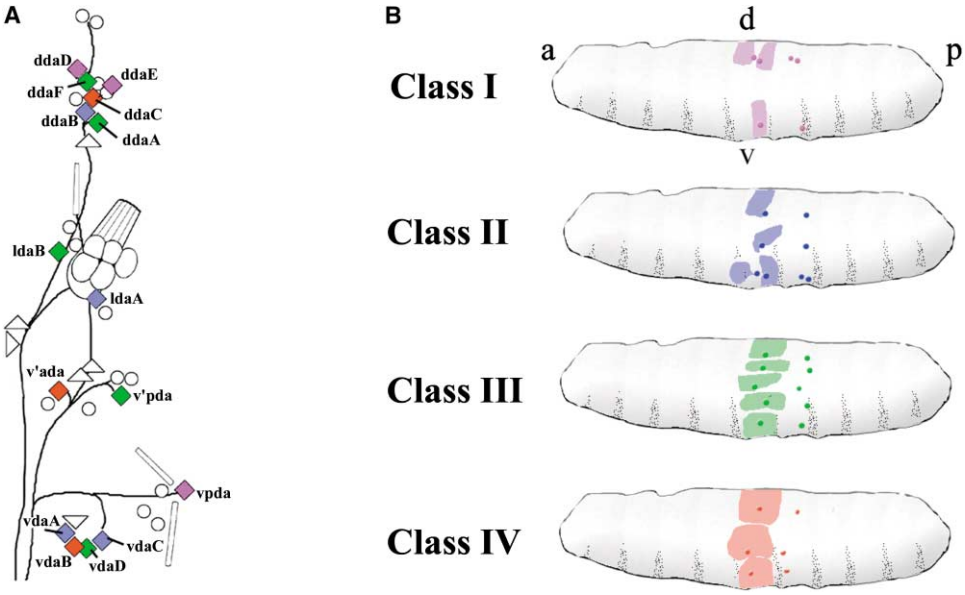

Figure 1. Arrangement of da Sensory Neurons and Their Dendritic Territories in the *Drosophila* Peripheral Nervous System

(A) A PNS schematic of a single abdominal hemisegment. da neurons of the same color have been placed in the same morphological class. (B) Arrangement of the territories of different da neuron classes along the larval body wall. The pattern shown is repeated in each abdominal hemisegment, although only two segments are schematized in this diagram (left segments with cell body and dendritic field indicated, and right segment with cell body only).

by using the MARCM system (for mosaic analysis with a repressible cell marker) [15]. Occasionally, two neighboring like neurons were labeled, but at too low frequency to permit systematic experimental investigations of tiling. To circumvent this limitation, we created transgenic flies with all class IV neurons labeled with EGFP. We found that the distribution of class IV neurons correlated well with the spatial arrangement of neurons expressing the *pickpocket* (*ppk*) gene [16, 17]. Reasoning that regions upstream of the *ppk* transcription initiation site might contain sequences required for class IV-specific expression, we fused 1-kb, 3-kb, and 6-kb genomic fragments with a minimal heat shock promoter and EGFP cDNA (Figure 2A). Indeed, the 1-kb and 3-kb fragments reproduced the reported pattern of *ppk* RNA and protein; although, low amounts of EGFP were also observed in the class III neurons. The 6-kb fragment drove expression in many additional cells in the head and in small numbers of cells adjacent to trachea. We used a 1-kb transformant line, *ppk-EGFP*^{5}, which harbors an insert on the third chromosome, for all subsequent analyses.

EGFP expression was detected first in the cell bodies of class IV neurons in stage-16 embryos (Figure 2B), and by early stage 17, the initial dendritic territories of each neuron were visible (Figure 2C). EGFP expression was maintained throughout larval stages (Figure 2D) and pupal stages (data not shown; C. Kuo and Y.N.J., unpublished data). Tiling was apparent in the ventral neurons, vdaB and v′ada, at around the time of hatching. The dorsal midline region was the last to become innervated, and dendrites did not cover this region until midway through the first larval stage (data not shown). Observations of late embryonic and early larval stages suggest that tiling is established as dendrites first meet, as we did not observe obvious overlap at any stage. Avoidance responses were also observed when branches within the same neuron (isoneuronal branches) met (Figure 2G). Once these borders were established, juxtaposed terminal dendrites remained dynamic. Imaging of branches at a 24-hr interval beginning in the second instar larval stage (n = 9 animals) revealed a net extension of both existing and new branches and a net change in the trajectory of others (Figures 2H and 2H′). This dynamic behavior is consistent with a requirement for continuous dendrite growth to maintain coverage of a body wall whose surface area is constantly expanding.

Consequences of Ablating Class IV Neuron Cell Bodies

The uniform, nonredundant innervation of the body wall by dendrites of class IV neurons, and the absence of gaps between neighboring fields, suggested that repulsive signaling might occur between heteroneuronal, in addition to isoneuronal, dendritic branches to minimize dendritic overlap. We tested this possibility by laser ablating single class IV neurons in stage-17 embryos and examining the fields of surrounding neurons 1, 2, or 3 days later (Figure 3). We found that class IV neurons extended dendrites into areas previously occupied by any neighboring cell that was ablated (Figures 3B–3D; n = 63). Dendritic invasion occurred across segments and also across the dorsal and ventral midlines (Figures 3C and 3D); this finding suggests that these boundaries do not limit dendrite growth at this stage. Furthermore, although dendrites invading from opposite sides of the ablated cell came into close proximity (Figure 3D), overlap was not observed, suggesting that cell pairs not

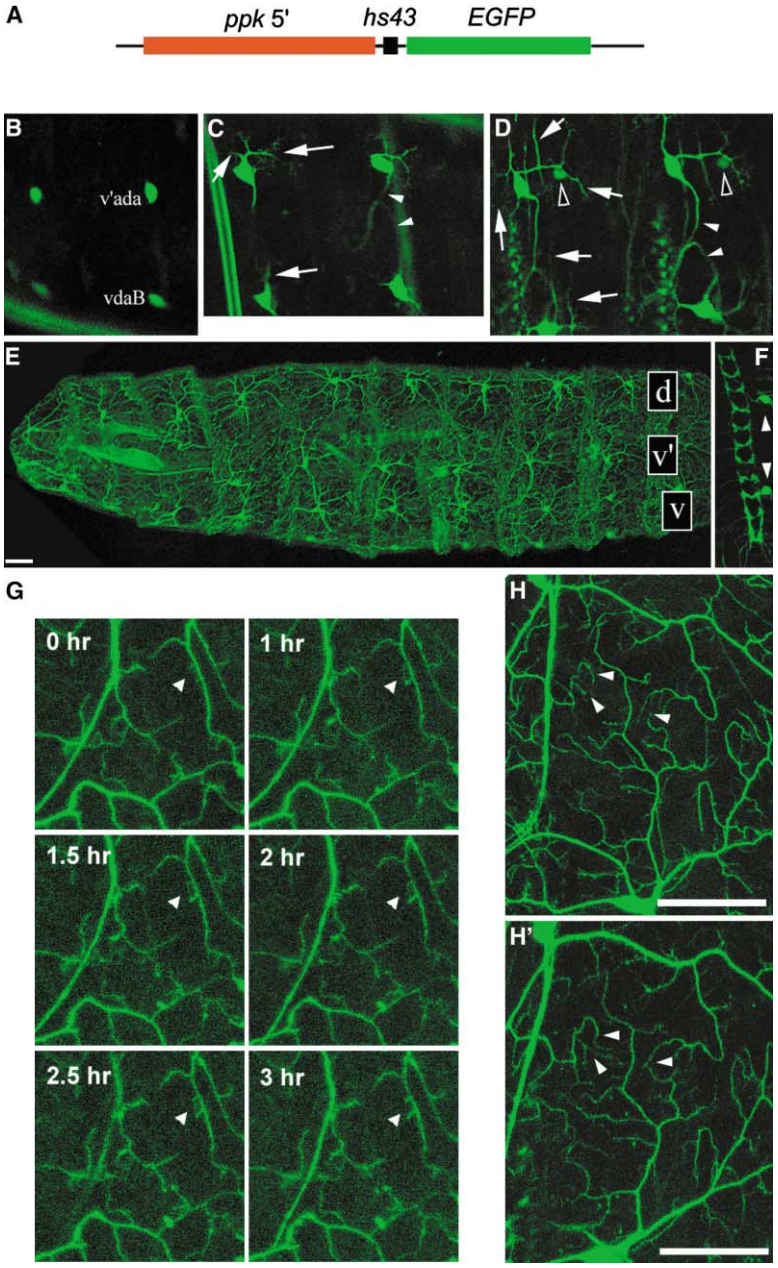

Figure 2. Labeling of Class IV Sensory Neurons by Using an Enhancer-EGFP Fusion Construct

(A) A schematic diagram of the *ppk* enhancer construct. Red indicates the enhancer region, black indicates the minimal heat shock promoter, and green indicates the EGFP cDNA.
(B) A stage-16 embryo showing EGFP expression in the segmentally repeated class IV neurons.
(C) An early stage-17 embryo showing EGFP in developing dendrites (arrows) and axons (arrowheads).
(D) A late stage-17 embryo with dendrites (arrows) and axons (white arrowheads). Note the weak labeling of class III neurons just posterior to the class IV neurons (black arrowheads).
(E) A second instar larva showing the segmentally repeated pattern of class IV neurons. The scale bar represents 100 μm.
(F) Labeling of the CNS is observed in the axon terminals of class IV neurons. The cell bodies of two ventral class IV neurons are indicated by arrowheads.
(G) Time-lapse of dendritic branches in early first instar (24 hr AEL). The time points at which the images were collected are indicated in the figures. Arrowheads indicate a point at which a branch extended toward, met with, and retracted from another branch of the same neuron (v′ada).
(H and H′) Time-lapse of the dendritic boundary formed by vdaB and v′ada dendrites beginning in the second instar (H) and again 24 hr later (H′). Several arbors have extended or reoriented over this time period (arrowheads in both figures). The scale bar represents 50 μm.

normally adjacent to each other are also capable of repulsion. To quantify the effects of ablation, we measured the maximum dendrite extension of neurons located adjacent to the ablated cell and compared this value to the dendritic extension of a segmental homolog (see bars in Figure 3D′). The mean ratio for class IV segmental homologs when no ablation was performed was 1.09 (± 0.19 SD, n = 38) (Figure 4A). Mean ratios after cell ablation fell between 1.3 and 4.2 (Figures 4B–4D). The highest values were for v′ada after ablation of vdaB (range from 1.7 to 10, n = 20), and the lowest values were for v′ada after ablation of ddaC (range from 1.2 to 1.4, n = 3) and for ddaC after ablation of its contralateral homolog (range from 1.5 to 1.8, n = 9). Thus, the same neuron, such as v′ada, can show different growth responses depending on which neighboring cell is ablated. These results suggest that selective ablation of class IV neurons in embryos eliminates a factor that normally acts to restrict growth of like dendrites.

The size of a *Drosophila* larva increases during development without the addition of new neurons to the da system. Nevertheless, the dendritic arbors of the class IV neurons maintain full coverage of the epidermis. The growth and remodeling of arbors at dendritic field boundaries (Figures 2H and 2H′) raised the possibility that repulsive signals might be required not only to establish, but also to maintain, a tiled body wall. To address this issue, we focused on the boundary formed by the dendrites of vdaB and v′ada, which was highly sensitive to cell ablation in embryonic stages (Figure

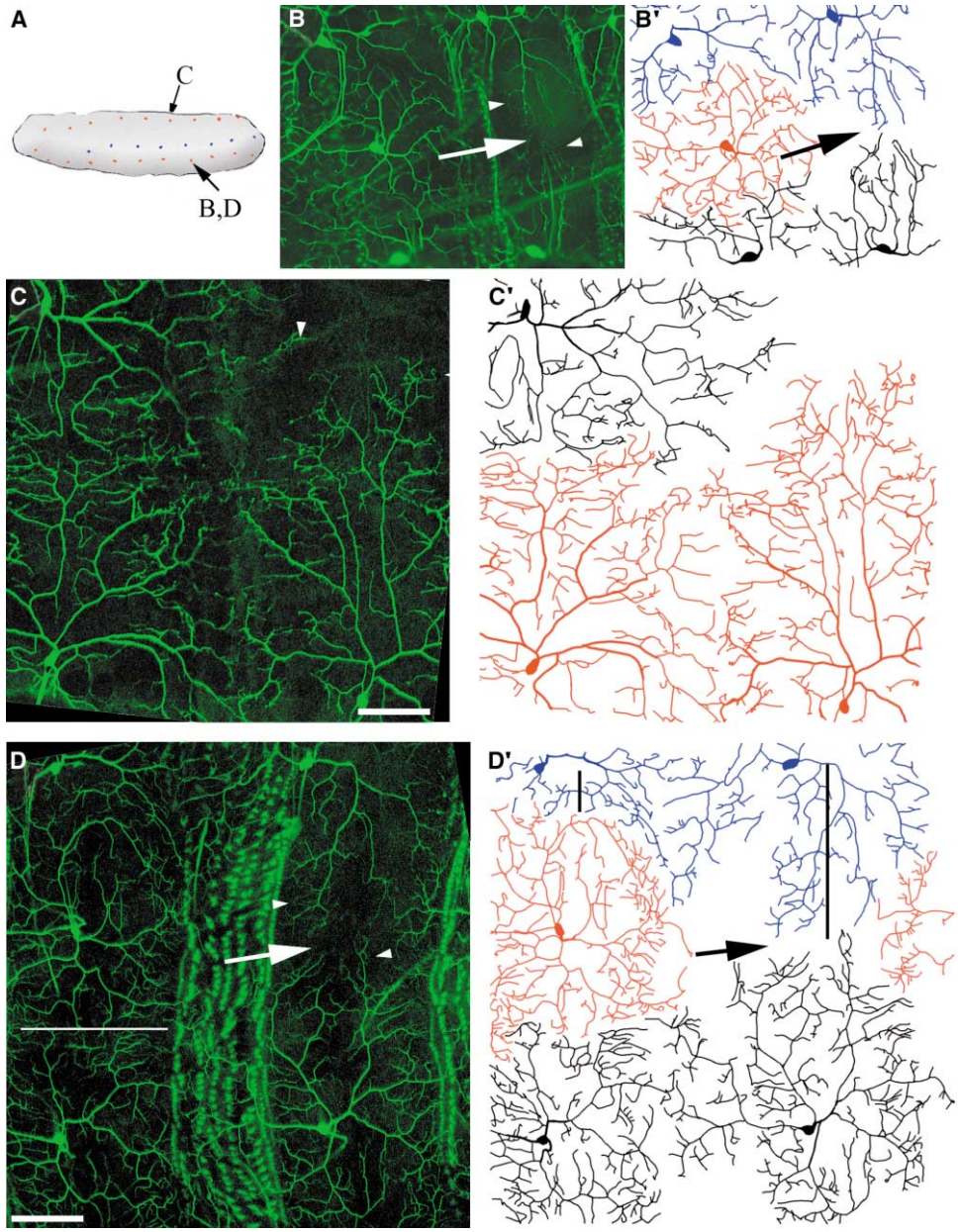

Figure 3. Effect of Embryonic Ablation of Class IV Neurons on the Dendritic Territories of Surrounding Like Neurons

(A) A schematic of the arrangement of class IV neurons. The ddaC neuron is colored red (top row of cells), the v′ada neuron is colored blue, and the vdaB neuron is colored red (bottom row of cells). Arrows indicate the positions of cells ablated in each subsequent panel. Anterior is oriented toward the left.

(B and B′) Embryonic ablation of vdaB (arrow) leads to dendritic invasion by v′ada and the vdaB neuron of the contralateral hemisegment (arrowheads) within 24 hr. Neurons from the contralateral hemisegment are colored black in (B′).

(C and C′) Third instar larva showing invasion of ddaC dendrites across the dorsal midline and segment border (arrowhead) after ablation of an adjacent homolog in the embryonic stage. Neurons from the contralateral hemisegment are colored black in (C′). The scale bar represents 100 μm.

(D and D′) Third instar larva showing growth of v′ada and vdaB (arrowheads) after ablation of vdaB (arrow). (D) The ventral midline is indicated by a thin white bar. (D′) Two vertical black bars show the path of dendrite growth used for quantitative analysis. Neurons from the contralateral hemisegment are colored black in (D′). The scale bar represents 100 μm.

4D). As in embryos, ablation of vdaB in second instar larvae led to enhanced ventral extension of v′ada dendrites ($n = 10$; Figure 5A). This ventral overextension was associated with the appearance of many fine branches oriented toward the ablated neuron (Figure 5A). Indeed, imaging of arbors immediately before cell ablation and again 24 hr later revealed oriented growth and branching of nascent, thin terminal branches at the border of the

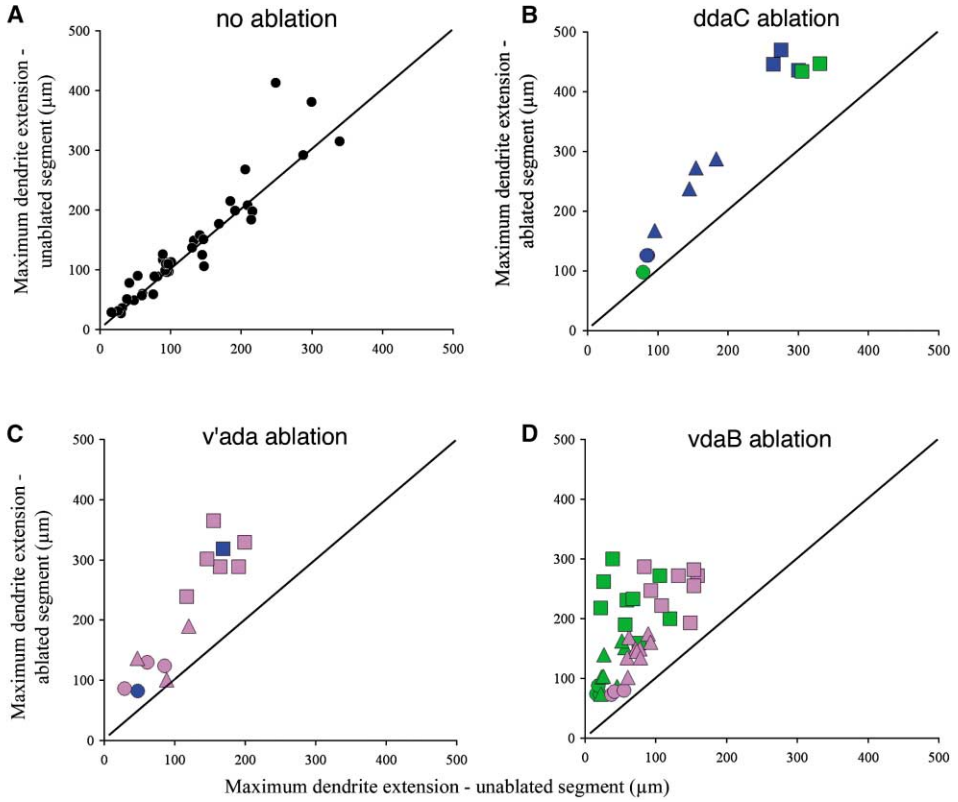

Figure 4. Quantification of the Effects of Cell Ablation in Embryonic Stages on Subsequent Dendritic Growth

(A) In the absence of cell ablation, homologous neurons from adjacent segments show similar maximum dendrite extensions. Each data point represents the ratio of segmentally homologous neurons in either first, second, or third instar larvae.

(B) Ablation of ddaC causes increased dendritic growth in the ablated segment relative to an adjacent unablated segment. Blue symbols indicate growth of ddaC; green symbols indicate growth of v′ada. For (B)–(D), circles represent data from first instar larvae, triangles represent data from second instar larvae, and squares represent data from third instar larvae.

(C) Ablation of v′ada causes increased growth of both vdaB (magenta symbols) and ddaC (blue symbols).

(D) Ablation of vdaB causes increased growth of both v′ada (green symbols) and vdaB (magenta symbols).

receptive field toward the ablated neuron (n = 5; Figure 5B). In contrast, major dendritic trunks, as well as secondary and many tertiary dendrites within the receptive field, appeared largely stable over this time period (Figure 5B).

Together, these experiments suggest that persistent repulsive signaling establishes a uniform and nonredundant dendritic coverage of the epidermis by altering the extent or trajectory of growth of homotypic branches.

Dendritic Field Alteration upon Duplication of Class IV Neurons

The growth of dendrites after cell ablation suggested that repulsive signaling is required for tiling. If these signals are communicated between dendrites, then overproduction of da neurons should lead to ectopic partitioning of territories. To test this idea, we induced an overproduction of class IV neurons by introducing mutations in the *hamlet* (*ham*) gene into a *ppk-EGFP* genetic background. *ham* is required for the specification of external sensory (es) neurons, and loss of *ham* leads to es neurons adopting a multidendritic neuron fate [18]. In a *ham* background, we frequently observed doubling of v′ada, but not of the other two abdominal class IV neurons. In each case (n = 11), the morphology of these two adjacent neurons was similar, and, in ten of these cases, dendrites projected to, and terminated within, distinct domains of the body wall (Figures 6A and 6B). We observed one case in which the major trunks of the two adjacent neurons clearly projected to an overlapping region, which the finer branches partitioned into nonoverlapping subdomains (data not shown). In response to the extra neuron, the dendritic field of vdaB was restricted to a more ventral region of the body wall (Figure 6B). The ectopic partitioning of the body wall induced by overproduction of class IV neurons strongly suggests that repulsive dendritic interactions occur between dendrites of like neurons.

Dendritic Fields of Duplicated Class I, II, and III Neurons

The class I, II, and III neurons are organized differently from the class IV neurons; they have dendrites that are either not normally in close apposition (classes I and II) or provide a low-density coverage of the body wall (class III). We asked whether these neurons might show exclusion if produced in excess. We produced supernumerary neurons by making MARCM clones by using *big brain*

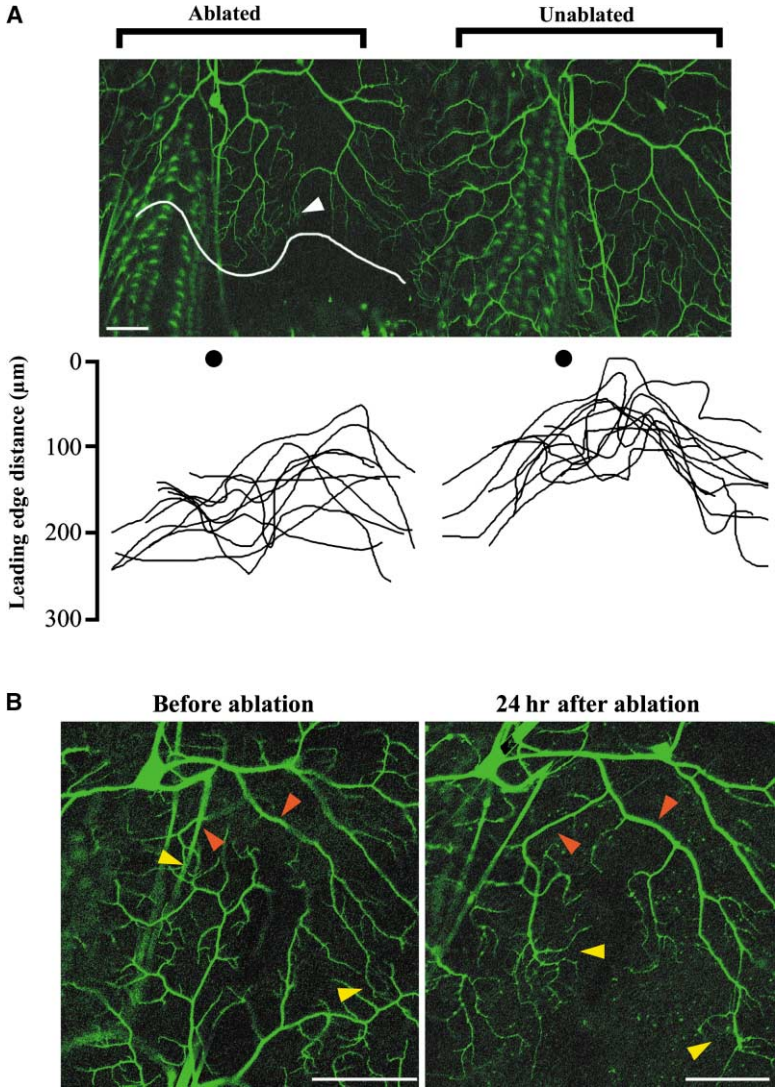

Figure 5. Effect of Cell Ablation in Larvae, after Dendritic Borders Are Established

(A) Top panel: comparison of dendritic territories of two v′ada neurons with and without ablation of vdaB. Note the more extensive fine branches extending from the cell adjacent to an ablated neuron (white arrowhead). A white line indicates the leading edge of the dendritic field. Bottom panel: cumulative plots of the distance from the cell body (circles) to the leading edge of the dendritic field (line) for all ablations (left) and an adjacent segment (right). The scale bar represents 50 μm.

(B) Preablation (left) and 24 hr postablation (right) images of the dendritic arbors of v′ada. Yellow arrowheads indicate regions in which dendrites grow toward the ablated neuron; red arrowheads indicate stable main branches. The scale bar represents 50 μm.

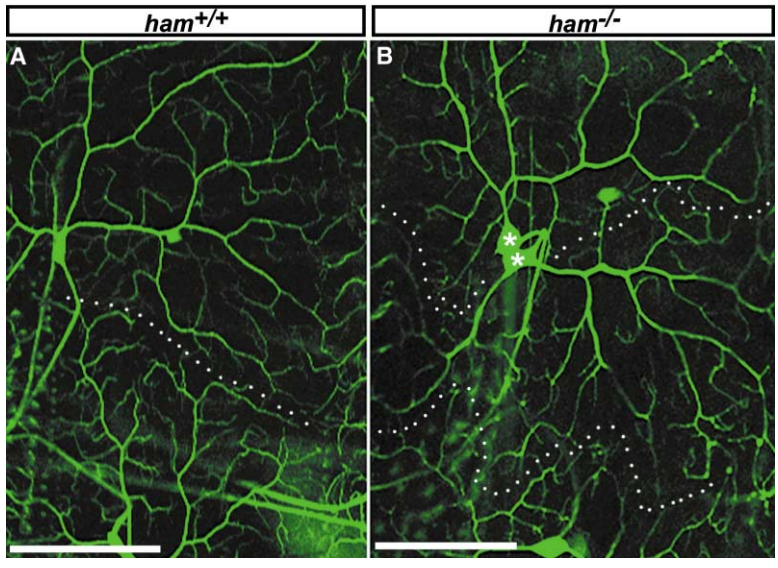

Figure 6. Partitioning of Territories by Supernumerary v′ada Neurons

(A) Tiling by v′ada (top) and vdaB (bottom). The boundary formed by dendrites is indicated by a dotted line. The scale bar represents 50 μm.

(B) Ectopic partitioning of territories after duplication of v′ada caused by mutation of the *hamlet* gene. White dotted lines indicate the positions of dendritic boundaries. The scale bar represents 50 μm.

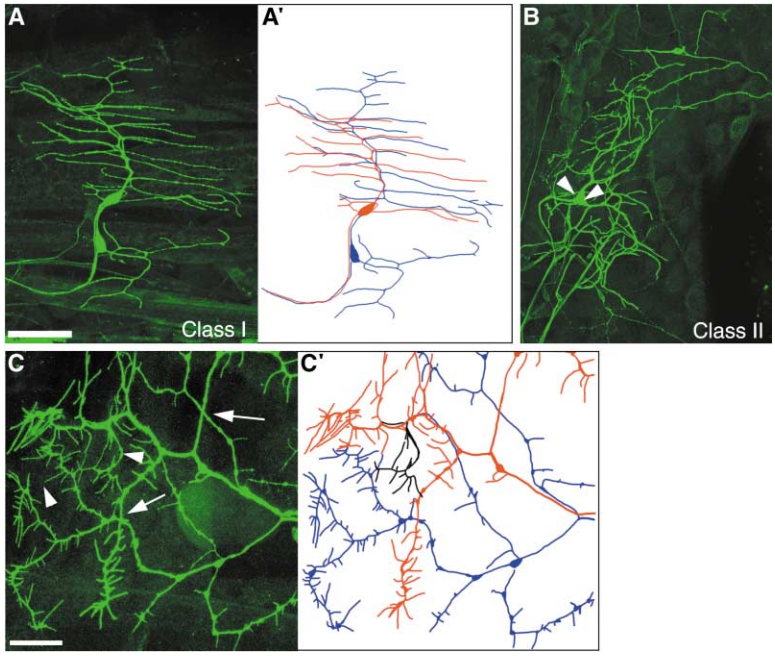

Figure 7. MARCM Analysis of the Effects of Overproduction of Class I, Class II, and Class III Neurons on Dendritic Territories of Like Neurons

(A and A′) Overproduction of vpda induced by mutation of *big brain*. (A′) Note the extensive overlap of primary and secondary dendrites. The scale bar represents 50 μm.

(B) Overproduction of the class II neuron, ldaA, induced by a mutation of the *hamlet* gene. The two cells, indicated by arrowheads, innervate the same territory.

(C and C′) Overproduction of the class III neuron, ldaB, induced by a mutation of the *hamlet* gene. Major trunk overlap is indicated by arrows. Exclusion of fine branches is indicated by arrowheads. (C′) Regions in which the identity of the arbor is ambiguous are drawn in black. The scale bar represents 25 μm.

(*bib*) [19] or *ham* mutations, both of which lead to overproduction of neurons. We observed duplications of class I, II, and III neurons in *ham* clones and of class I neurons in *bib* clones. In contrast to the dendritic avoidance exhibited by duplicated class IV neurons, duplicated class I neurons (n = 7 duplications) and class II neurons (n = 5 duplications) innervated overlapping regions of the body wall in each case examined (Figures 7A and 7B). Although these dendrites did not clearly fasciculate, they intermixed very extensively, and we often could not distinguish between the arbors of the two neurons (Figure 7B). Class III neurons duplicated in *ham* MARCM clones behaved much like the class I and II neurons in that their major trunks overlapped extensively and often extended along the same direction as they covered identical territories of the epidermis (n = 15 duplications; Figure 7C). Extensive overlap was not observed, however, among the short terminal extensions of the class III neurons (Figures 7C and 7C′). It is therefore possible that these short branches contribute to the dendritic exclusion normally observed among class III neurons.

Discussion

Developing dendrites progress through several stages, including outgrowth, extension and branching, and, eventually, cessation of growth and demarcation of a mature territory [20, 21]. Coordinated regulation of these processes is likely important for establishing the mature arbor morphologies that characterize particular classes of neurons. Territories may be defined by the intrinsic growth capacity of dendrites, or by extrinsic signals, such as physical barriers or repulsive signals from like dendrites. We have exploited the highly stereotyped territories and morphologies of *Drosophila* da sensory neurons to examine the cellular basis of dendritic territory formation.

Results from several recent studies suggest that dendritic interactions between da neurons regulate the size and shape of dendritic fields. Ablation of a cluster of da neurons results in overgrowth of dendrites from adjacent hemisegments [14]. Subsequent studies showed that the neurons within these clusters are morphologically diverse [7, 22] and that only those sharing a similar morphology consistently innervate exclusive territories [7]. These results suggested that dendritic interactions might show type selectivity. Our present results from ablation and addition-of-neuron experiments suggest that repulsive dendritic interactions indeed occur between branches of like neurons to regulate dendritic field sizes, but they also indicate that neurons can show diverse responses to like dendrites. In particular, we observed a fairly strict dendritic exclusion among the class IV neurons, whereas dendrites of supernumerary class I, II, and III neurons overlapped extensively with dendrites of resident same-class neurons (Figure 7). Thus, like-repels-like signaling may be a property only of neurons that provide a complete coverage of a receptive territory and, even among these neurons, may be restricted to specific regions of the dendritic arbor. How are dendritic fields defined among neurons that appear not to employ homotypic repulsion? Possibly, different types of neurons have different intrinsic growth capacitites determined by their expression of particular cell identity factors. Other growth-limiting factors might include genes that, when mutated, cause overgrowth phenotypes, such as *flamingo* [14] and *sequoia* [23], or as yet unidentified extrinsic limitations to dendrite extension.

The da system of *Drosophila* shows notable similarities to and differences from other systems, such as the vertebrate retina and leech somatosensory system, in which tiling and interbranch repulsion have been studied. Destruction of small patches of retinal ganglion cells (RGCs) causes neighboring dendrites to grow preferen-

tially toward the depleted area [9]. Dendritic tiling by RGCs may generally involve interactions between dendrites of adjacent cells [2, 11]. This exclusion appears to occur independently of afferent inputs to RGC dendrites [24]. Thus, even though da neuron dendrites are unlike RGC dendrites in that they have no known synaptic inputs, they may prove useful for identifying conserved mechanisms of dendrodendritic interaction. In the leech also, proper innervation of peripheral targets by pressure, touch, and nociceptive neurons requires both intra- and interneuronal interactions between sensory fibers [25–27]. Anatomical and ablation studies in leech suggest that exclusion is most rigorous between different branches of the same neuron, less strict between homologous cells, and weak or absent if cells are of a different modality [25, 27]. The overlap of arbors of duplicated neurons, but not of branches belonging to the same neuron (Figure 7), may reflect such a hierarchy in the da system. The contrasting behaviors of isoneuronal and heteroneuronal branches of class I, II, and III neurons suggest that mechanisms of avoidance may differ for "self" and "non-self" branches. It is also possible that isoneuronal and heteroneuronal repulsion share some common molecular mechanism, but that physical continuity of arbors contributes to a more strict avoidance by isoneuronal branches [28].

Several properties of the signals regulating tiling are implied in our results. Firstly, the interaction between dendrites seems to be inhibitory and can result in the turning of dendrites and/or the cessation of dendrite extension. Secondly, it is likely that the interaction is bidirectional. In other words, it is unlikely that one dendrite is only capable of sending out the signal while the other dendrite can only receive the signal. Lastly, because interactions occur between like dendrites and are required persistently, at least some molecules are likely to show a class-specific distribution in embryonic and larval stages. With the high resolution provided by the *ppk-EGFP* lines, it is feasible to carry out both candidate-based approaches and unbiased genetic screens to identify molecules involved in dendrodendritic interaction and tiling.

Experimental Procedures

Fly Stocks

The following stocks were used for MARCM experiments in this study: *w elav-Gal4, hsFLP, UAS-mCD8::GFP/FM7*; *tubP-Gal80, FRT40A/CyO* [18], *ham*^{1} *FRT40A/CyO* [18], and *y w;* P[*y*+], *bib*^{IDO5}, *ck, FRT40A/CyO, ftz-lacZ*. For overproduction of class IV neurons, *ham*^{1} was crossed transiently into a *ppk-EGFP* background.

Construction of Transgenic Lines

A SacI/EcoRI fragment (~6 kb) from BAC clone 21J17, which contains the putative enhancer region of the *ppk* gene, was identified by Southern analysis and then subcloned. PCR reactions were carried out to generate a 3-kb and a 1-kb fragment by using this SacI/EcoRI fragment as a template. The transformation vector pCasper-hs43-lacZ was modified by replacing the reporter gene *lacZ* with a cDNA encoding EGFP (Clontech) to generate a new vector, pCasper-hs43-EGFP. The *ppk* genomic fragments were then inserted into a region immediately upstream of the minimal heat shock promoter of pCasper-hs43-EGFP. These constructs were injected into *w*^{1118} embryos [29] together with a DNA construct encoding the transposase Δ*2-3*. Multiple independent lines carrying inserts on either chromosome 2 or chromosome 3 were generated with the 6-kb, 3-kb, and 1-kb constructs.

Cell Ablation Experiments and Image Analysis

To ablate *EGFP*-expressing cells in embryonic stages, adults were allowed to lay eggs on a grape agar plate for 2 hr, then the eggs were allowed to develop until approximately 17 hr after egg laying (AEL) at 25°C. Eggs were dechorionated in 100% bleach and were arranged on an agar dish so that the region of the PNS to be targeted was facing down. A 22 × 50 coverslip with double-stick tape along its length and pieces of colored tape acting as spacers along each side was lightly placed over these embryos, inverted, and covered with Series 27 halocarbon oil. A second coverslip was then placed over these embryos prior to ablation. Ablation was carried out on a Micropoint Laser System (Photonic Instruments) with a 337 nm pulsed nitrogen laser. During ablation, we observed fluorescence quenching within the nucleus, but not the cytoplasm, of targeted cells. We did not observe obvious damage to the epidermis; however, some damage immediately underneath ablated neurons cannot be ruled out.

To ablate cells in larval stages, second instar larvae were placed on a slide and covered with a small amount of halocarbon oil. Larvae were covered with a 22 × 22 mm glass coverslip, and single neurons were ablated as described above. We found that, when placed in a modest amount of halocarbon oil, larvae moved only minimally under the coverslip and therefore did not require anesthetics.

For successive imaging of larvae before and after ablation, we placed individual larvae on a glass slide covered in halocarbon oil. A coverslip with a tape spacer was gently placed on top of the larva so that it was immobilized but not compressed enough to burst. A Leica TCS-SP2 confocal microscope was set on four line scan mode, and, because the dendrites of class IV neurons approximate a planar surface, single images were acquired from the ventral region of segment A2. The coverslip was floated away by placing the slide in a dish of halocarbon oil, and the larva was allowed to recover for between 1 and 3 hr. Individual neurons were then laser ablated as described above, the larvae returned to 25°C to develop for 24 hr, and the neurons reimaged.

For time-lapse analysis of early larval stages, eggs of *ppk-EGFP* flies were collected for 2 hr at 25°C and were allowed to develop for 24 hr. Early first instar larvae were immersed in 80% glycerol and were covered with a coverslip. Time-lapse images were collected with confocal microscopy. To minimize the chance of missing parts of dendritic branches in optic sectioning, a series of images across the *z* axis were collected at each time point such that the thickness of each optic section was less than 1 μm. In addition, the total thickness of each series was much greater than the thickness of the dendritic trees.

Acknowledgments

We thank Cynthia Kenyon for use of the cell ablation equipment, Joy Alcedo for expert advice on its use, and Mike Rothenberg for advice on making transgenic animals. We thank Tadashi Uemura for discussing data prior to publication. This work was supported by National Institutes of Health (NIH) 1R01 NS 40929-0 to Y.N.J, NIH T32 NS007-067-23 and 1 F32 NS43027-01A1 to W.G., NIH T32 NS007-067-24 to B.Y., and a Wellcome Trust Traveling Fellowship to A.M. L.Y.J. and Y.N.J. are Investigators of the Howard Hughes Medical Institute.

Received: November 22, 2002
Revised: February 3, 2003
Accepted: February 20, 2003
Published: April 15, 2003

References

1. Wässle, H., and Reimann, H.J. (1978). The mosaic of nerve cells in the mammalian retina. Proc. R. Soc. Lond. B Biol. Sci. *200*, 441–461.
2. Wässle, H., Peichl, L., and Boycott, B.B. (1981). Dendritic territories of cat retinal ganglion cells. Nature *292*, 344–345.

3. Wässle, H., and Boycott, B.B. (1991). Functional architecture of the mammalian retina. Physiol. Rev. *71*, 447–478.
4. Amthor, F.R., and Oyster, C.W. (1995). Spatial organization of retinal information about the direction of image motion. Proc. Natl. Acad. Sci. USA *92*, 4002–4005.
5. Galli-Resta, L. (1998). Patterning the vertebrate retina: the early appearance of retinal mosaics. Semin. Cell Dev. Biol. *9*, 279–284.
6. MacNeil, M.A., and Masland, R.H. (1998). Extreme diversity among amacrine cells: implications for function. Neuron *20*, 971–982.
7. Grueber, W.B., Jan, L.Y., and Jan, Y.N. (2002). Tiling of the *Drosophila* epidermis by multidendritic sensory neurons. Development *129*, 2867–2878.
8. Sestan, N., Artavanis-Tsakonas, S., and Rakic, P. (1999). Contact-dependent inhibition of cortical neurite growth mediated by notch signaling. Science *286*, 741–746.
9. Perry, V.H., and Linden, R. (1982). Evidence for dendritic competition in the developing retina. Nature *297*, 683–685.
10. Leventhal, A.G., Schall, J.D., and Ault, S.J. (1988). Extrinsic determinants of retinal ganglion cell structure in the cat. J. Neurosci. *8*, 2028–2038.
11. Hitchcock, P.F. (1989). Exclusionary dendritic interactions in the retina of the goldfish. Development *106*, 589–598.
12. Weber, A.J., Kalil, R.E., and Stanford, L.R. (1998). Dendritic field development of retinal ganglion cells in the cat following neonatal damage to visual cortex: evidence for cell class specific interactions. J. Comp. Neurol. *390*, 470–480.
13. Bodmer, R., and Jan, Y.N. (1987). Morphological differentiation of the embryonic peripheral neurons in *Drosophila*. Roux's Arch. Dev. Biol. *196*, 69–77.
14. Gao, F.B., Kohwi, M., Brenman, J.E., Jan, L.Y., and Jan, Y.N. (2000). Control of dendritic field formation in *Drosophila*: the roles of Flamingo and competition between homologous neurons. Neuron *28*, 91–101.
15. Lee, T., and Luo, L. (1999). Mosaic analysis with a repressible cell marker for studies of gene function in neuronal morphogenesis. Neuron *22*, 451–461.
16. Adams, C.M., Anderson, M.G., Motto, D.G., Price, M.P., Johnson, W.A., and Welsh, M.J. (1998). Ripped pocket and pickpocket, novel *Drosophila* DEG/ENaC subunits expressed in early development and mechanosensory neurons. J. Cell Biol. *140*, 143–152.
17. Darboux, I., Lingueglia, E., Pauron, D., Barbry, P., and Lazdunski, M. (1998). A new member of the amiloride-sensitive sodium channel family in *Drosophila melanogaster* peripheral nervous system. Biochem. Biophys. Res. Commun. *246*, 210–216.
18. Moore, A.W., Jan, L.Y., and Jan, Y.N. (2002). *hamlet*, a binary genetic switch between single- and multiple-dendrite neuron morphology. Science *297*, 1355–1358.
19. Rao, Y., Bodmer, R., Jan, L.Y., and Jan, Y.N. (1992). The *big brain* gene of *Drosophila* functions to control the number of neuronal precursors in the peripheral nervous system. Development *116*, 31–40.
20. Scott, E.K., and Luo, L. (2001). How do dendrites take their shape? Nat. Neurosci. *4*, 359–365.
21. Jan, Y.N., and Jan, L.Y. (2001). Dendrites. Genes Dev. *15*, 2627–2641.
22. Sweeney, N.T., Li, W., and Gao, F.B. (2002). Genetic manipulation of single neurons *in vivo* reveals specific roles of Flamingo in neuronal morphogenesis. Dev. Biol. *247*, 76–88.
23. Brenman, J.E., Gao, F.B., Jan, L.Y., and Jan, Y.N. (2001). Sequoia, a tramtrack-related zinc finger protein, functions as a pan-neuronal regulator for dendrite and axon morphogenesis in *Drosophila*. Dev. Cell *1*, 667–677.
24. Perry, V.H., and Maffei, L. (1988). Dendritic competition: competition for what? Brain Res. *41*, 195–208.
25. Nicholls, J.G., and Baylor, D.A. (1968). Specific modalities and receptive fields of sensory neurons in the CNS of the leech. J. Neurophysiol. *31*, 740–756.
26. Blackshaw, S.E., Nicholls, J.G., and Parnas, I. (1982). Expanded receptive fields of cutaneous mechanoreceptor cells after single neuron deletion in the leech central nervous system. J. Physiol. *326*, 261–268.
27. Gan, W.B., and Macagno, E.R. (1995). Interactions between segmental homologs and between isoneuronal branches guide the formation of sensory terminal fields. J. Neurosci. *15*, 3243–3253.
28. Wang, H., and Macagno, E.R. (1998). A detached branch stops being recognized as self by other branches of a neuron. J. Neurobiol. *35*, 53–64.
29. Rubin, G.M., and Spradling, A.C. (1982). Genetic transformation of *Drosophila* with transposable element vectors. Science *218*, 348–353.